Outage Constrained Robust Beamforming for Secure Broadcasting Systems With Energy Harvesting

Zhengyu Zhu, *Student Member, IEEE*, Zheng Chu, Zhongyong Wang, *Member, IEEE*, and Inkyu Lee, *Fellow, IEEE*

***Abstract*— In this paper, we investigate simultaneous wireless information and power transfer systems for multiuser multiple-input single-output secure broadcasting channels. Considering imperfect channel state information, we introduce a robust secure beamforming design, where the transmit power is minimized subject to the secrecy rate outage probability constraint for legitimate users and the harvested energy outage probability constraint for energy harvesting receivers. The original problem is non-convex due to the presence of the probabilistic constraints. With the aid of Bernstein-type inequalities, we transform the outage constraints into the deterministic forms. Based on a successive convex approximation (SCA) method, we propose a low-complexity approach, which reformulates the original problem as a second-order cone programming problem. Also, we prove the convergence of the SCA-based iterative algorithm. Simulation shows that the proposed scheme outperforms the conventional method with lower complexity.**

***Index Terms*— SWIPT, physical-layer secrecy, outage probability, robust optimization, successive convex approximation.**

I. INTRODUCTION

RECENTLY, energy harvesting (EH) techniques have been introduced which extracts energy from the nature. The EH can be applied to avert energy-limited issues and enhance energy efficiency of wireless networks [1]–[4]. However, the natural energy sources such as solar power and wind are climate dependent and cannot provide stable energy to portable wireless devices in practice [5], [6]. Due to a serious path loss, wireless power transfer (WPT) be feasible only for short distance. To overcome the attenuation over distance, radio frequency (RF) enabled WPT has been employed for sustaining low power device, such as RFID (radio frequency identification) and wireless sensors [7]. Recent green technologies significantly promote the WPT efficiency, by utilizing MIMO method [8]. Leveraging the fact that ambient radio frequency (RF) signals can carry energy while transporting information, simultaneous wireless information and power transfer (SWIPT) has been proposed which utilizes the RF-enabled signal generating power to wireless networks [9]–[14], [17].

On the other hand, security [15], [16] has been recognized as an important issue for SWIPT systems [18]–[30]. To address this security problem, physical layer security techniques have been applied to SWIPT to achieve secure communication [18]. In [19], the optimal beamforming designs for secrecy SWIPT systems in multiple-input single-output (MISO) broadcast channels were studied. Also, a secure beamforming scheme for SWIPT in non-regenerative relay networks was examined in [20]. Moreover, the secure transmission for SWIPT schemes was investigated in cooperative networks [21], multiple-input multiple-output (MIMO) broadcasting systems [22], wireless fading channels [23], and distributed antenna networks [24].

It is worth noting that all of these works have assumed that perfect channel state information (CSI) is available at the transmitter. However, due to channel estimation and quantization errors, it may be difficult to attain perfect CSI at the transmitter in practice. Some secure transmission methods with wiretap channels in MISO SWIPT broadcast systems were presented under imperfect CSI in [25]–[30]. However, these works only adopted the norm-bounded channel uncertainty model [25]–[30], which may not reflect practical channels accurately, since the channel error bound cannot be obtained exactly.

In practice, an outage constrained robust method is more flexible where CSI errors are modeled as random variables. Unfortunately, a problem with outage constraint may not have a close-form solution and is almost impossible to be dealt with in a direct manner. To overcome this issue, a conservative probability inequality approximation that can guarantee the satisfaction of the outage constraints has been applied

Manuscript received November 11, 2015; revised May 30, 2016; accepted August 20, 2016. Date of publication September 1, 2016; date of current version November 9, 2016. This work was supported in part by the China National 863 Project under Grant 2014AA01A705, in part by the National Nature Science Foundation of China under Grant 61571402, Grant 61172086, Grant 61571401, Grant 61401401, Grant 61301150, and Grant 61501404, in part by the Specialized Research Fund for the Doctoral Program of Higher Education under Grant 20134101120001, in part by the Outstanding Young Talent Research Fund of Zhengzhou University under Grant 1521318003, in part by the China Postdoctoral Science Foundation under Grant 2015T80779, in part by the Newton Fund/British Council Institutional Links under Grant 101977, and in part by the National Research Foundation of Korea (NRF) funded by the Korea Government (MSIP) under Grant 2014R1A2A1A10049769. The associate editor coordinating the review of this paper and approving it for publication was S. Jin.

Z. Zhu is with the School of Information Engineering, Zhengzhou University, Zhengzhou 450001, China, and also with the School of Electrical Engineering, Korea University, Seoul 136-713, South Korea (e-mail: zhuzhengyu6@gmail.com).

Z. Chu was with the School of Electrical and Electronic Engineering, Newcastle University, Newcastle upon Tyne, NE1 7RU, U.K. He is now with the School of Science and Technology, Middlesex University, London, NW4 4BT, U.K. (e-mail: z.chu@ncl.ac.uk).

Z. Wang is with the School of Information Engineering, Zhengzhou University, Zhengzhou 450001, China (e-mail: iezywang@zzu.edu.cn).

I. Lee is with the School of Electrical Engineering, Korea University, Seoul 136-713, South Korea (e-mail: inkyu@korea.ac.kr).

Color versions of one or more of the figures in this paper are available online at http://ieeexplore.ieee.org.

Digital Object Identifier 10.1109/TWC.2016.2605102

in [31]–[33]. In several works [10]–[34], [37], [39]–[41], a semi-definite relaxation (SDR) technique has been widely used in various tramsmit beamforming design problems, where a convex semi-definite programming (SDP) approximation was directly generated. In general, the relaxed problem is not guaranteed to obtain a rank-one solution and always acts as a performance upper bound for the original problem [34]. In addition, the proof of a rank-two solution of the transmit covariance matrix was presented in [28]–[30], which may not be correct. Since it is challenging to show a rank-one solution, a suboptimal solution was only provided by adopting a conventional Gaussian randomization (GR) method [28]–[30], [34] or a constrained concave convex procedure (CCCP)-based scheme proposed in [36] and [37]. Nevertheless, one main disadvantage of both techniques is its poor performance when the SDP returns a high-rank transmit precoding matrix.

Unlike conventional GR and CCCP-based methods, to avoid rank relaxation, the successive convex approximation (SCA) technique [38] can provide a high-quality approximate transmit beamforming solution via solving a set of convex problems. Due to the complicated nonconvex outage constraints in multiuser MISO interference channels in the SCA algorithm, the original problem is successively approximated to a convex form and the transmit beamforming solution is achieved in an iterative manner [39]. In [40], the SDR method was studied for a robust sum rate maximization problem in two-way relay systems with energy harvesting, in which the SCA technique is employed to get a Karush-Kuhn-Tucker (KKT) solution efficiently.

Motivated by the aforementioned observations, in this paper, we consider a system where only the statistical information of channel uncertainties is available at the transmitter. We incorporate two different types of statistical channel uncertainty models which are more realistic compared to the norm-bound channel uncertainty in [28]–[30]: 1) partial channel uncertainties which assume perfect CSI for legitimate users and imperfect CSI for eavesdroppers and EH receivers and 2) full channel uncertainties which consider imperfect CSI for legitimate users, eavesdroppers and EH receivers.

We formulate a robust transmit power minimization (PM) problem subject to the secrecy rate outage probability constraint for legitimate users and the harvested power outage probability constraint for EH receivers for both channel uncertainty models. Under various assumptions on the CSI, we seek to design robust transmit beamforming strategies for MISO SWIPT wiretap channels. The main contributions of this paper are summarized as follows:

- For the two different types of statistical channel uncertainty models, the robust PM problem with the outage constraints is converted into a problem with deterministic form constraint by employing the Bernstein-type inequality [31].
- For the partial channel uncertainty model, by utilizing a successive convex approximation (SCA) method, the recast PM problem is transformed to a second order cone programming (SOCP) problem, which can be directly solved to obtain a local optimal solution.
- For the full channel uncertainty model, the SCA method can also be employed to convert the concave constraint into the liner constraint. Then, applying the Cauchy-Schwarz inequality, the recast PM problem is transformed again into an SOCP problem for which we can efficiently obtain a high-quality approximate solution.

It is shown analytically that the proposed SOCP-SCA algorithm efficiently produces a beamforming solution with lower that is a stationary point for the SDR of the original problem. The outage-constrained PM problem with a fixed secrecy rate target was discussed in [32] assuming that a distribution of CSI errors is known, and a SDP algorithm was proposed to get a feasible rank-one solution. However, it is not possible to extend the results in [32] to general cases with multiple legitimate user and EH receivers which are considered in this paper.

The rest of this paper is organized as follows: Section II presents the system model. In Section III, the statistical channel uncertainty model and the problem formulation are provided. Robust design methods are developed in Section IV. Section V compares the computational complexity of the proposed robust design methods and the conventional schemes, and Section VI illustrates the simulation results. Finally, we conclude the paper in Section VII.

Notation: Vectors and matrices are denoted by bold lowercase and uppercase letters, respectively. $(\cdot)^H$ represents the Hermitian transpose. For a vector $\boldsymbol{x}$, $\|\boldsymbol{x}\|$ indicates the Euclidean norm. $|\cdot|$ defines the absolute value of a complex scalar. $\mathbb{C}^{M\times L}$ and $\mathbb{H}^{M\times L}$ describe the space of $M\times L$ complex matrices and Hermitian matrices, respectively. For a matrix $\mathbf{A}$, $\mathbf{A}\succeq\mathbf{0}$ means that $\mathbf{A}$ is positive semi-definite, $\|\mathbf{A}\|_F$ and $\mathrm{tr}(\mathbf{A})$ indicate the Frobenius norm and trace, respectively, and $vec(\mathbf{A})$ stacks the elements of $\mathbf{A}$ in a column vector. $\mathrm{E}\{\cdot\}$ describes the mathematical expectation. $\Re\{\cdot\}$ stands for the real part of a complex number. $[x]^+$ equals $\max\{x,0\}$. $\lambda_{max}(\mathbf{A})$ denotes the maximum eigenvalue of $\mathbf{A}$.

II. System Model

In this section, we consider a MISO secure broadcasting channel with SWIPT, which consists of one multi-antenna transmitter, K legitimate users, L eavesdroppers, and U EH receiver. It is assumed that the transmitter is equipped with M_{T} transmit antennas, whereas legitimate users, eavesdroppers and EH receivers have a single receive antenna.

The channel vectors from the transmitter to the k-th legitimate user, the l-th eavesdropper and the u-th EH receiver are denoted by $\boldsymbol{h}_{s,k}\in\mathbb{C}^{M_{\mathrm{T}}\times 1}$, $\boldsymbol{h}_{e,l}\in\mathbb{C}^{M_{\mathrm{T}}\times 1}$, and $\boldsymbol{h}_{h,u}\in\mathbb{C}^{M_{\mathrm{T}}\times 1}$, respectively. Then, the received signal at the k-th legitimate user, the l-th eavesdropper and the u-th EH receiver can be written as

$$\begin{aligned} y_{s,k} &= \boldsymbol{h}_{s,k}^H\boldsymbol{w}s + n_{s,k}, \quad \text{for } k=1,\ldots,K,\\ y_{e,l} &= \boldsymbol{h}_{e,l}^H\boldsymbol{w}s + n_{e,l}, \quad \text{for } l=1,\ldots,L,\\ y_{h,u} &= \boldsymbol{h}_{h,u}^H\boldsymbol{w}s, \quad \text{for } u=1,\ldots,U, \end{aligned} \tag{1}$$

where $\boldsymbol{w}\in\mathbb{C}^{M_{\mathrm{T}}\times 1}$ indicates the transmit beamforming vector at the transmitter, s is the desired data intended for the legitimate user satisfying $\mathbb{E}\left\{|s|^2\right\}=1$, and $n_{s,k}\sim\mathcal{CN}(0,\sigma_{s,k}^2)$

and $n_{e,l} \sim \mathcal{CN}(0, \sigma_{e,l}^2)$ represent the noise at the k-th legitimate user and the l-th eavesdropper, respectively. Here, the transmitter is assumed to know the noise variance and the number of receive antenna equipped at the eavesdroppers. Specifically, we only focus on single-cell systems and ignore co-channel interference caused by frequency reuse. Thus, the achieved secrecy rate at the k-th legitimate user is expressed as

$$R_{s,k} = \left[\log(1+\frac{|\boldsymbol{h}_{s,k}^H\boldsymbol{w}|^2}{\sigma_{s,k}^2}) - \max_l \log(1+\frac{|\boldsymbol{h}_{e,l}^H\boldsymbol{w}|^2}{\sigma_{e,l}^2})\right]^+, \quad \forall k. \tag{2}$$

Also, the harvested energy at the u-th EH receiver is written as $E_u = \zeta_u \left|\boldsymbol{h}_{h,u}^H\boldsymbol{w}\right|, \forall u$ where $0 < \zeta_u \leq 1$ is the energy conversion efficiency. For simplicity, we assume $\zeta_u = 1$.

III. Statistical Channel Uncertainty and Problem Formulation

In this section, we investigate a robust beamforming design for systems with statistical channel uncertainties. First, we introduce two scenarios of the channel uncertainties, and then provide the problem formulation based on the channel uncertainties.

A. Partial Channel Uncertainty (PCU)

In this scenario, we assume that the transmitter has perfect knowledge of the legitimate user's CSI, while CSI of eavesdroppers and the EH receivers is imperfect due to channel errors. Normally, the CSI of the legitimate user is easier to obtain compared to that of an eavesdropper, since it is often learned through reliable training and feedback [32]. Here, the channel vectors of the eavesdroppers and the EH receivers are written as

$$\begin{aligned} \boldsymbol{h}_{e,l} &= \hat{\boldsymbol{h}}_{e,l} + \Delta\boldsymbol{h}_{e,l}, \text{ for } \ l = 1, \ldots, L, \\ \boldsymbol{h}_{h,u} &= \hat{\boldsymbol{h}}_{h,u} + \Delta\boldsymbol{h}_{h,u}, \text{ for } u = 1, \ldots, U, \end{aligned} \tag{3}$$

where $\hat{\boldsymbol{h}}_{e,l} \in \mathbb{C}^{M_{\mathrm{T}}}$ and $\hat{\boldsymbol{h}}_{h,u} \in \mathbb{C}^{M_{\mathrm{T}}}$ are the estimated channel vectors, and $\Delta\boldsymbol{h}_{e,l}$ and $\Delta\boldsymbol{h}_{h,u}$ denote the channel errors modeled as zero-mean Gaussian random variables with covariance $\mathbf{E}_{e,l}$ and $\mathbf{E}_{h,u}$, respectively, i.e., $\Delta\boldsymbol{h}_{e,l} \sim \mathcal{CN}(0, \mathbf{E}_{e,l})$ and $\Delta\boldsymbol{h}_{h,u} \sim \mathcal{CN}(0, \mathbf{E}_{h,u})$. Then, the CSI uncertainty vector $\Delta\boldsymbol{h}_{e,l}$ and $\Delta\boldsymbol{h}_{h,u}$ can be expressed as $\Delta\boldsymbol{h}_{e,l} = \mathbf{E}_{e,l}^{\frac{1}{2}}\tilde{\boldsymbol{h}}_{e,l}$ and $\Delta\boldsymbol{h}_{h,u} = \mathbf{E}_{h,u}^{\frac{1}{2}}\tilde{\boldsymbol{h}}_{h,u}$ where $\tilde{\boldsymbol{h}}_{e,l} \sim \mathcal{CN}(0, \mathbf{I}_{M_{\mathrm{T}}})$ and $\tilde{\boldsymbol{h}}_{h,u} \sim \mathcal{CN}(0, \mathbf{I}_{M_{\mathrm{T}}})$ [35].

B. Full Channel Uncertainty (FCU)

In this scenario, we consider the case of imperfect CSI for legitimate users, eavesdroppers and EH receivers. Thus, in addition to the channels models in (3), the channel vector for the legitimate users is determined as

$$\boldsymbol{h}_{s,k} = \hat{\boldsymbol{h}}_{s,k} + \Delta\boldsymbol{h}_{s,k}, \text{ for } \ k = 1, \ldots, K, \tag{4}$$

where $\hat{\boldsymbol{h}}_{s,k} \in \mathbb{C}^{M_{\mathrm{T}}}$ is the estimated channel vector, and $\Delta\boldsymbol{h}_{s,k}$ represents the channel errors following a distribution $\Delta\boldsymbol{h}_{s,k} \sim \mathcal{CN}(0, \mathbf{E}_{s,k})$. Then, the CSI uncertainty vector $\Delta\boldsymbol{h}_{s,k}$ can be given as $\Delta\boldsymbol{h}_{s,k} = \mathbf{E}_{s,k}^{\frac{1}{2}}\tilde{\boldsymbol{h}}_{s,k}$ where $\tilde{\boldsymbol{h}}_{s,k} \sim \mathcal{CN}(0, \mathbf{I}_{M_{\mathrm{T}}})$.

In this paper, our aim is to minimize the transmit power subject to the secrecy rate outage constraint and the harvested energy outage constraint. Based on the above uncertainty models, the robust outage optimization problem is formulated as

$$\min_{\boldsymbol{w}} \quad \|\boldsymbol{w}\|^2 \tag{5a}$$

$$s.t. \ \Pr\{R_{s,k} \geq \bar{R}\} \geq 1 - \rho_{k,l}, \ \forall k, l, \tag{5b}$$

$$\Pr\{\left|\boldsymbol{h}_{h,u}^H\boldsymbol{w}\right| \geq \bar{E}\} \geq 1 - \rho_u, \tag{5c}$$

where $\bar{R} > 0$ and $\bar{E} > 0$ are the given secrecy rate target for all the legitimate users and the harvested power target for EH receivers, respectively, and $\rho_{k,l} \in (0, 1]$ and $\rho_u \in (0, 1]$ indicate the maximal outage probability of the secrecy rate and the harvested power, respectively.

The outage constrained problem (5a) is known to be computationally intractable [43]. The main challenge of problem (5a) lies in the outage probability constraint (5b) and (5c), which do not allow simple close-form expressions. In the conventional methods [31], [32], the semidefinite relaxation (SDR) technique was employed to the robust outage-constrained problem as an SDP problem by rank relaxation. It is noted that solving the SDP problem requires high computational complexity and may result in relatively poor performance if SDP returns a high-rank solution. In the following, we will propose a SCA-based robust design method for overcoming this challenge in problem (5a).

IV. Proposed Robust Designs

A. Partial Channel Uncertainty

In this subsection, we propose a robust design method for systems where perfect CSI for legitimate users is known to the transmitter. First, the Bernstein-type inequality is applied to convert the outage constraint into the deterministic form. Also, the SCA method is employed to convexify the concave part of a convex-concave function via restriction approximation techniques [38]–[40], [43], [47]. Then, utilizing SOCP relaxation, we reformulate the PM problem (5a) as an SOCP problem and develop an SOCP-SCA method to obtain a local optimal beamforming solution.

First, we derive the secrecy rate outage probability in (5b) as

$$\begin{aligned} &\Pr\{\log\left(1+\frac{|\boldsymbol{h}_{s,k}^H\boldsymbol{w}|^2}{\sigma_{s,k}^2}\right) - \log\left(1+\frac{|(\hat{\boldsymbol{h}}_{e,l}+\Delta\boldsymbol{h}_{e,l})^H\boldsymbol{w}|^2}{\sigma_{e,l}^2}\right) \geq \bar{R}\} \\ &= \Pr\{\Delta\boldsymbol{h}_{e,l}^H\boldsymbol{w}\boldsymbol{w}^H\Delta\boldsymbol{h}_{e,l} + 2\Re\{\Delta\boldsymbol{h}_{e,l}^H\boldsymbol{w}\boldsymbol{w}^H\hat{\boldsymbol{h}}_{e,l}\} + \hat{\boldsymbol{h}}_{e,l}^H\boldsymbol{w}\boldsymbol{w}^H\hat{\boldsymbol{h}}_{e,l} \\ &\leq \frac{2^{-\bar{R}}\sigma_{e,l}^2}{\sigma_{s,k}^2}\left(\sigma_s^2 + \boldsymbol{h}_{s,k}^H\boldsymbol{w}\boldsymbol{w}^H\boldsymbol{h}_{s,k}\right) - \sigma_{e,l}^2\}. \end{aligned}$$

Then, the secrecy rate outage constraint (5b) is given as

$$\begin{aligned} \Pr\Big\{&\tilde{\boldsymbol{h}}_{e,l}^H\mathbf{E}_{e,l}^{\frac{1}{2}}\boldsymbol{w}\boldsymbol{w}^H\mathbf{E}_{e,l}^{\frac{1}{2}}\tilde{\boldsymbol{h}}_{e,l} + 2\Re\{\tilde{\boldsymbol{h}}_{e,l}^H\mathbf{E}_{e,l}^{\frac{1}{2}}\boldsymbol{w}\boldsymbol{w}^H\hat{\boldsymbol{h}}_{e,l}\} + \hat{\boldsymbol{h}}_{e,l}^H\boldsymbol{w}\boldsymbol{w}^H\hat{\boldsymbol{h}}_{e,l} \\ &- \frac{2^{-\bar{R}}\sigma_{e,l}^2}{\sigma_{s,k}^2}\left(\sigma_{s,k}^2 + \boldsymbol{w}^H\boldsymbol{h}_{s,k}\boldsymbol{h}_{s,k}^H\boldsymbol{w}\right) + \sigma_{e,l}^2 \geq 0\Big\} \\ &\leq \rho_{k,l}, \quad \forall k, l. \end{aligned} \tag{6}$$

Also, the harvested energy outage probability in (5c) can be rewritten as

$$\begin{aligned}
&\Pr\left\{|\boldsymbol{h}_{h,u}\boldsymbol{w}|^2 \geq \bar{E}\right\}\\
&= \Pr\left\{\Delta\boldsymbol{h}_{h,u}^H\boldsymbol{w}\boldsymbol{w}^H\Delta\boldsymbol{h}_{h,u} + 2\Re\{\Delta\boldsymbol{h}_{h,u}^H\boldsymbol{w}\boldsymbol{w}^H\hat{\boldsymbol{h}}_{h,u}\}\right.\\
&\qquad \left. + \hat{\boldsymbol{h}}_{h,u}^H\boldsymbol{w}\boldsymbol{w}^H\hat{\boldsymbol{h}}_{h,u} \geq \bar{E}\right\}\\
&= \Pr\left\{\tilde{\boldsymbol{h}}_{h,u}^H\mathbf{E}_{h,u}^{\frac{1}{2}}\boldsymbol{w}\boldsymbol{w}^H\mathbf{E}_{h,u}^{\frac{1}{2}}\tilde{\boldsymbol{h}}_{h,u} + 2\Re\{\tilde{\boldsymbol{h}}_{h,u}^H\mathbf{E}_{h,u}^{\frac{1}{2}}\boldsymbol{w}\boldsymbol{w}^H\hat{\boldsymbol{h}}_{h,u}\}\right.\\
&\qquad \left. + \hat{\boldsymbol{h}}_{h,u}^H\boldsymbol{w}\boldsymbol{w}^H\hat{\boldsymbol{h}}_{h,u} \geq \bar{E}\right\},\ \forall u.
\end{aligned}$$

Thus, we can convert the outage constraint (5c) into

$$\begin{aligned}
&\Pr\left\{\tilde{\boldsymbol{h}}_{h,u}^H\mathbf{E}_{h,u}^{\frac{1}{2}}\boldsymbol{w}\boldsymbol{w}^H\mathbf{E}_{h,u}^{\frac{1}{2}}\tilde{\boldsymbol{h}}_{h,u} + 2\Re\{\tilde{\boldsymbol{h}}_{h,u}^H\mathbf{E}_{h,u}^{\frac{1}{2}}\boldsymbol{w}\boldsymbol{w}^H\hat{\boldsymbol{h}}_{h,u}\}\right.\\
&\qquad \left. + \hat{\boldsymbol{h}}_{h,u}^H\boldsymbol{w}\boldsymbol{w}^H\hat{\boldsymbol{h}}_{h,u} \geq \bar{E}\right\} \geq 1-\rho_u,\ \forall u. \qquad (7)
\end{aligned}$$

Here, (6) and (7) are still outage constraints and are hard to deal with. Now, we apply the Bernstein-type inequalities [31] to provide a conservative approximation of (6) and (7).

Lemma 1 (Bernstein-Type Inequalities): Assuming that $\boldsymbol{f} \in \mathbb{C}^{n\times 1}$ is distributed as $\mathcal{CN}(0, \mathbf{I})$, consider $g(\boldsymbol{f}) = \boldsymbol{f}^H\mathbf{U}\boldsymbol{f} + 2\Re\{\boldsymbol{u}^H\boldsymbol{f}\}$, where $\mathbf{U} \in \mathbb{H}^{n\times n}$ and $\boldsymbol{u} \in \mathbb{C}^{n\times 1}$. Then for any nonnegative number $\sigma \in (0, 1]$, we have

$$\Pr\{g(\boldsymbol{f}) \geq \mathrm{tr}(\mathbf{U}) + \sqrt{2\delta(\|\mathbf{U}\|_F^2 + 2\|\boldsymbol{u}\|^2)} + \sigma s^+(\mathbf{U})\} \leq e^{-\sigma},$$

$$\Pr\{g(\boldsymbol{f}) \leq \mathrm{tr}(\mathbf{U}) - \sqrt{2\delta(\|\mathbf{U}\|_F^2 + 2\|\boldsymbol{u}\|^2)} - \sigma s^-(\mathbf{U})\} \leq e^{-\sigma},$$

where $s^+(\mathbf{U}) = \max\{\lambda_{\max}(\mathbf{U}), 0\}$, and $s^-(\mathbf{U}) = \max\{\lambda_{\max}(-\mathbf{U}), 0\}$. ■

Adopting Lemma 1, we change the outage constraints (6) and (7) into the deterministic form as

$$\boldsymbol{w}^H(\hat{\boldsymbol{h}}_{e,l}\hat{\boldsymbol{h}}_{e,l}^H + \mathbf{E}_{e,l})\boldsymbol{w} + s_{k,l} \leq \frac{2^{-\bar{R}}\sigma_{e,l}^2}{\sigma_{s,k}^2}\boldsymbol{w}^H\boldsymbol{h}_{s,k}\boldsymbol{h}_{s,k}^H\boldsymbol{w}, \qquad (8a)$$

$$\sqrt{\left\|\mathbf{E}_{e,l}^{\frac{1}{2}}\boldsymbol{w}\boldsymbol{w}^H\mathbf{E}_{e,l}^{\frac{1}{2}}\right\|_F^2 + 2\left\|\mathbf{E}_{e,l}^{\frac{1}{2}}\boldsymbol{w}\boldsymbol{w}^H\hat{\boldsymbol{h}}_{e,l}\right\|^2} \leq q_{k,l}, \qquad (8b)$$

$$p_{k,l}\mathbf{I} - \mathbf{E}_{e,l}^{\frac{1}{2}}\boldsymbol{w}\boldsymbol{w}^H\mathbf{E}_{e,l}^{\frac{1}{2}} \succeq \mathbf{0},\ \ p_{k,l} \geq 0,\ \forall k, l, \qquad (8c)$$

$$\boldsymbol{w}^H(\mathbf{E}_{h,u} + \hat{\boldsymbol{h}}_{h,u}\hat{\boldsymbol{h}}_{h,u}^H)\boldsymbol{w} \geq \sqrt{-2\ln\rho_u}n_u - m_u\ln\rho_u + \bar{E}, \qquad (9a)$$

$$\sqrt{\left\|\mathbf{E}_{h,u}^{\frac{1}{2}}\boldsymbol{w}\boldsymbol{w}^H\mathbf{E}_{h,u}^{\frac{1}{2}}\right\|_F^2 + 2\left\|\mathbf{E}_{h,u}^{\frac{1}{2}}\boldsymbol{w}\boldsymbol{w}^H\hat{\boldsymbol{h}}_{h,u}\right\|^2} \leq n_u, \qquad (9b)$$

$$m_u\mathbf{I} + \mathbf{E}_{h,u}^{\frac{1}{2}}\boldsymbol{w}\boldsymbol{w}^H\mathbf{E}_{h,u}^{\frac{1}{2}} \succeq \mathbf{0}, m_u \geq 0,\ \forall u, \qquad (9c)$$

where $\{p_{k,l}\}$, $\{q_{k,l}\}$, n_u, and m_u are slack variables and $s_{k,l} = \sqrt{-2\ln\rho_{k,l}}q_{k,l} - p_{k,l}\ln\rho_{k,l} + \sigma_{e,l}^2 - 2^{-\bar{R}}\sigma_{e,l}^2$.

It is observed that $\boldsymbol{w}^H\boldsymbol{h}_{s,k}\boldsymbol{h}_{s,k}^H\boldsymbol{w}$ and $\boldsymbol{w}^H(\mathbf{E}_{h,u} + \hat{\boldsymbol{h}}_{h,u}\hat{\boldsymbol{h}}_{h,u}^H)\boldsymbol{w}$ are the concave part of constraints (8a) and (9a). First, we examine the first constraint of (8) and (9). Introducing a variable $t_{k,l}$, we can rewrite (8a) as

$$\boldsymbol{w}^H(\hat{\boldsymbol{h}}_{e,l}\hat{\boldsymbol{h}}_{e,l}^H + \mathbf{E}_{e,l})\boldsymbol{w} + s_{k,l} \leq t_{k,l}, \qquad (10a)$$

$$\frac{2^{-\bar{R}}\sigma_{e,l}^2}{\sigma_{s,k}^2}\boldsymbol{w}^H\boldsymbol{h}_{s,k}\boldsymbol{h}_{s,k}^H\boldsymbol{w} \geq t_{k,l}. \qquad (10b)$$

Then, we employ the SCA technique for the second-order cones (SOC) constraints (9a) and (10b) to achieve convex approximations.

Let $\boldsymbol{w}_0$ be an initial feasible point. Then, substituting $\boldsymbol{w} \triangleq \boldsymbol{w}_0 + \Delta\boldsymbol{w}$ into the left-hand side of (9a) and (10b), we can get

$$\begin{aligned}
&\boldsymbol{w}^H(\mathbf{E}_{h,u} + \hat{\boldsymbol{h}}_{h,u}\hat{\boldsymbol{h}}_{h,u}^H)\boldsymbol{w}\\
&\quad = (\boldsymbol{w}_0 + \Delta\boldsymbol{w})^H(\mathbf{E}_{h,u} + \hat{\boldsymbol{h}}_{h,u}\hat{\boldsymbol{h}}_{h,u}^H)(\boldsymbol{w}_0 + \Delta\boldsymbol{w})\\
&\quad \geq \boldsymbol{w}_0^H(\mathbf{E}_{h,u} + \hat{\boldsymbol{h}}_{h,u}\hat{\boldsymbol{h}}_{h,u}^H)\boldsymbol{w}_0\\
&\qquad\qquad + 2\Re\{\boldsymbol{w}_0^H(\mathbf{E}_{h,u} + \hat{\boldsymbol{h}}_{h,u}\hat{\boldsymbol{h}}_{h,u}^H)\Delta\boldsymbol{w}\}, \qquad (11)\\
&\boldsymbol{w}^H\boldsymbol{h}_{s,k}\boldsymbol{h}_{s,k}^H\boldsymbol{w}\\
&\quad = (\boldsymbol{w}_0 + \Delta\boldsymbol{w})^H\boldsymbol{h}_{s,k}\boldsymbol{h}_{s,k}^H(\boldsymbol{w}_0 + \Delta\boldsymbol{w})\\
&\quad \geq \boldsymbol{w}_0^H\boldsymbol{h}_{s,k}\boldsymbol{h}_{s,k}^H\boldsymbol{w}_0 + 2\Re\{\boldsymbol{w}_0^H\boldsymbol{h}_{s,k}\boldsymbol{h}_{s,k}^H\Delta\boldsymbol{w}\}, \qquad (12)
\end{aligned}$$

where (11) and (12) are derived by dropping the quadratic form $\Delta\boldsymbol{w}^H(\mathbf{E}_h + \hat{\boldsymbol{h}}_h\hat{\boldsymbol{h}}_h^H)\Delta\boldsymbol{w}$ and $\Delta\boldsymbol{w}^H\boldsymbol{h}_{s,k}\boldsymbol{h}_{s,k}^H\Delta\boldsymbol{w}$, respectively. According to (11) and (12), we then obtain linear approximations of the concave constraints (9a) and (10b) as

$$\begin{aligned}
&\boldsymbol{w}_0^H(\mathbf{E}_{h,u} + \hat{\boldsymbol{h}}_{h,u}\hat{\boldsymbol{h}}_{h,u}^H)\boldsymbol{w}_0 + 2\Re\{\boldsymbol{w}_0^H(\mathbf{E}_{h,u} + \hat{\boldsymbol{h}}_{h,u}\hat{\boldsymbol{h}}_{h,u}^H)\Delta\boldsymbol{w}\}\\
&\qquad \geq \sqrt{-2\ln\rho_u}n_u - m_u\ln\rho_u + \bar{E}, \qquad (13a)
\end{aligned}$$

$$\frac{2^{-\bar{R}}\sigma_{e,l}^2}{\sigma_{s,k}^2}(\boldsymbol{w}_0^H\boldsymbol{h}_{s,k}\boldsymbol{h}_{s,k}^H\boldsymbol{w}_0 + 2\Re\{\boldsymbol{w}_0^H\boldsymbol{h}_{s,k}\boldsymbol{h}_{s,k}^H\Delta\boldsymbol{w}\}) \geq t_{k,l}. \qquad (13b)$$

Next, we check the second constraint of (8) and (9a). To change into the convex form, their equivalent forms are given as

$$\begin{aligned}
&\sqrt{\left\|\mathbf{E}_{e,l}^{\frac{1}{2}}\boldsymbol{w}\boldsymbol{w}^H\mathbf{E}_{e,l}^{\frac{1}{2}}\right\|_F^2 + 2\left\|\mathbf{E}_{e,l}^{\frac{1}{2}}\boldsymbol{w}\boldsymbol{w}^H\hat{\boldsymbol{h}}_{e,l}\right\|^2}\\
&\quad = \sqrt{\boldsymbol{w}^H\mathbf{E}_{e,l}\boldsymbol{w}\boldsymbol{w}^H(\mathbf{E}_{e,l} + \hat{\boldsymbol{h}}_{e,l}\hat{\boldsymbol{h}}_{e,l}^H)\boldsymbol{w}} \leq q_{k,l}, \forall k, l, \qquad (14a)\\
&\sqrt{\left\|\mathbf{E}_{h,u}^{\frac{1}{2}}\boldsymbol{w}\boldsymbol{w}^H\mathbf{E}_{h,u}^{\frac{1}{2}}\right\|_F^2 + 2\left\|\mathbf{E}_{h,u}^{\frac{1}{2}}\boldsymbol{w}\boldsymbol{w}^H\hat{\boldsymbol{h}}_{h,u}\right\|^2}\\
&\quad = \sqrt{\boldsymbol{w}^H\mathbf{E}_{h,u}\boldsymbol{w}\boldsymbol{w}^H(\mathbf{E}_{h,u} + \hat{\boldsymbol{h}}_{h,u}\hat{\boldsymbol{h}}_{h,u}^H)\boldsymbol{w}} \leq n_u, \forall u. \qquad (14b)
\end{aligned}$$

Introducing x_l, y_l, a_u, and b_u are slack variables, we can express the above inequations (14a) and (14b) as

$$\boldsymbol{w}^H\mathbf{E}_{e,l}\boldsymbol{w} \leq e^{2x_l}, \qquad (15a)$$

$$\boldsymbol{w}^H(\mathbf{E}_{e,l} + \hat{\boldsymbol{h}}_{e,l}\hat{\boldsymbol{h}}_{e,l}^H)\boldsymbol{w} \leq e^{2y_l}, \qquad (15b)$$

$$e^{x_l+y_l} \leq q_{k,l}, \qquad (15c)$$

$$\boldsymbol{w}^H\mathbf{E}_{h,u}\boldsymbol{w} \leq e^{2a_u}, \qquad (16a)$$

$$\boldsymbol{w}^H(\mathbf{E}_{h,u} + \hat{\boldsymbol{h}}_{h,u}\hat{\boldsymbol{h}}_{h,u}^H)\boldsymbol{w} \leq e^{2b_u}, \qquad (16b)$$

$$e^{a_u+b_u} \leq n_u. \qquad (16c)$$

Let us define $x_l(q)$, $y_l(q)$, $a_u(q)$, and $b_u(q)$ as the variables x_l, y_l, a_u, and b_u at the q-th iteration for an SCA iterative algorithm. By employing an approximate expression $e^{x_l(q)}(x_l - x_l(q) + 1) \leq e^{x_l}$, we transform the non-convex constraint (15) and (15d) to their corresponding convex

Algorithm 1 Proposed SOCP-SCA Robust Design

Set the iteration number $q = 0$ and initialize $\boldsymbol{w}_0$ as a feasible point.

Repeat

- Solve problem (20) with $\boldsymbol{w}_q$ and denote a solution $\boldsymbol{w}$ by $\boldsymbol{w}^*$.
- Set $\boldsymbol{w}_{q+1} = \boldsymbol{w}^*$ and update the iteration number $q \leftarrow q + 1$.

Until Convergence

approximations as

$$\boldsymbol{w}^H \mathbf{E}_{e,l} \boldsymbol{w} \le e^{2x_l(q)}(2x_l - 2x_l(q) + 1), \tag{17a}$$

$$\boldsymbol{w}^H (\mathbf{E}_{e,l} + \hat{\boldsymbol{h}}_{e,l}\hat{\boldsymbol{h}}_{e,l}^H)\boldsymbol{w} \le e^{2y_l(q)}(2y_l - 2y_l(q) + 1), \tag{17b}$$

$$e^{x_l + y_l} \le q_{k,l}, \tag{17c}$$

$$\boldsymbol{w}^H \mathbf{E}_{h,u} \boldsymbol{w} \le e^{2a_u(q)}(2a_u - 2a_u(q) + 1), \tag{18a}$$

$$\boldsymbol{w}^H (\mathbf{E}_{h,u} + \hat{\boldsymbol{h}}_{h,u}\hat{\boldsymbol{h}}_{h,u}^H)\boldsymbol{w} \le e^{2b_u(q)}(2b_u - 2b_u(q) + 1), \tag{18b}$$

$$e^{a_u + b_u} \le n_u. \tag{18c}$$

At last, we consider the third constraints of (8) and (9a). The constraint (8c) $p_{k,l}\mathbf{I} - \mathbf{E}_{e,l}^{\frac{1}{2}} \boldsymbol{w}\boldsymbol{w}^H \mathbf{E}_{e,l}^{\frac{1}{2}} \succeq \mathbf{0}$ is equivalent to

$$\boldsymbol{w}^H \mathbf{E}_{e,l} \boldsymbol{w} \le p_{k,l}. \tag{19}$$

Also, it is easy to see that the constraint (8i) $m_u\mathbf{I} + \mathbf{E}_{h,u}^{\frac{1}{2}} \boldsymbol{w}\boldsymbol{w}^H \mathbf{E}_{h,u}^{\frac{1}{2}} \succeq \mathbf{0}$ is valid. According to equations from (6) to (19), we propose an SOCP-SCA robust design iterative algorithm. Let us denote $\boldsymbol{w}_q$ as a given transmit beamforming solution obtained at the q-th iteration. At the $(q+1)$-th iteration, problem (5a) can be thus reformed as

$$\min_{\boldsymbol{w}, \{p_{k,l}\}, \{q_{k,l}\}, \{t_{k,l}\}, \{n_u\}, \{m_u\}, \{x_l\}, \{y_l\}, \{a_u\}, \{b_u\}} \|\boldsymbol{w}\|$$
$$s.t.\ (10a),\ (13),\ (17),\ (17d),\ (19),\ \Delta\boldsymbol{w} = \boldsymbol{w} - \boldsymbol{w}_q. \tag{20}$$

Problem (20) is an SOCP problem and can be directly solved by CVX tools which are more efficient than SDP [42]. Suppose that $\boldsymbol{w}_q^*$ is the optimal solution at the q-th iteration. Then, The optimal solution $\boldsymbol{w}_{q+1}^*$ is updated as $\boldsymbol{w}_{q+1}^* = \boldsymbol{w}_q^*$ until the algorithm converges. We summarize the SOCP-SCA robust design in Algorithm 1. Note that the iterative SCA algorithm may have a convergence issue as the approximation counterparts may cause divergence. Now, we prove the convergence property of Algorithm 1 in the following theorem.

Theorem 1: Denoting $f_q^*(\boldsymbol{w}_q^*)$ as the optimal objective at the q-th iteration, we have $f_q^*(\boldsymbol{w}_q^*) \ge f_{q+1}^*(\boldsymbol{w}_{q+1}^*)$. Thus, as q grows, $\|\Delta\boldsymbol{w}\|$ approaches 0 and Algorithm 1 will converge.

Proof: See Appendix A. ■

B. Full Channel Uncertainty (FCU)

In this subsection, we consider the case where all the channel knowledge are imperfect. We will extend our robust design in the previous subsection to the case where only a distribution of all CSI is available at the transmitter. By considering all the channel uncertainties in (4), the secrecy rate outage probability in (5b) can be written as

$$\begin{aligned}
&\Pr\Big\{ \log\big(1 + \frac{|(\hat{\boldsymbol{h}}_{s,k} + \Delta\boldsymbol{h}_{s,k})^H \boldsymbol{w}|^2}{\sigma_{s,k}^2}\big) \\
&\quad - \log\big(1 + \frac{|(\hat{\boldsymbol{h}}_{e,l} + \Delta\boldsymbol{h}_{e,l})^H \boldsymbol{w}|^2}{\sigma_{e,l}^2}\big) \ge \bar{R} \Big\} \\
&= \Pr\Big\{ \frac{1}{\sigma_{s,k}^2} \Delta\boldsymbol{h}_{s,k}{}^H \boldsymbol{w}\boldsymbol{w}^H \Delta\boldsymbol{h}_{s,k} + \frac{2}{\sigma_{s,k}^2} \Re\{\Delta\boldsymbol{h}_{s,k}^H \boldsymbol{w}\boldsymbol{w}^H \hat{\boldsymbol{h}}_{s,k}\} \\
&\quad + \frac{1}{\sigma_{s,k}^2} \hat{\boldsymbol{h}}_{s,k}^H \boldsymbol{w}\boldsymbol{w}^H \hat{\boldsymbol{h}}_{s,k} - \frac{2^{\bar{R}}}{\sigma_{e,l}^2} \Delta\boldsymbol{h}_{e,l}{}^H \boldsymbol{w}\boldsymbol{w}^H \Delta\boldsymbol{h}_{e,l} \\
&\quad - \frac{2^{\bar{R}+1}}{\sigma_{e,l}^2} \Re\{\Delta\boldsymbol{h}_{e,l}^H \boldsymbol{w}\boldsymbol{w}^H \hat{\boldsymbol{h}}_{e,l}\} - \frac{2^{\bar{R}}}{\sigma_{e,l}^2} \hat{\boldsymbol{h}}_{e,l}^H \boldsymbol{w}\boldsymbol{w}^H \hat{\boldsymbol{h}}_{e,l} \ge 2^{\bar{R}} - 1 \Big\} \\
&= \Pr\{\Delta\boldsymbol{h}_{k,l}^H \bar{\mathbf{W}} \Delta\boldsymbol{h}_{k,l} + 2\Re\{\Delta\boldsymbol{h}_{k,l}^H \bar{\mathbf{W}} \hat{\boldsymbol{h}}_{k,l}\} + \hat{\boldsymbol{h}}_{k,l}^H \bar{\mathbf{W}} \hat{\boldsymbol{h}}_{k,l} \\
&\quad \ge 2^{\bar{R}} - 1\},
\end{aligned} \tag{21}$$

where $\Delta\boldsymbol{h}_{k,l} = \begin{bmatrix} \Delta\boldsymbol{h}_{s,k}^T & \Delta\boldsymbol{h}_{e,l}^T \end{bmatrix}^T$, $\bar{\mathbf{W}} = \operatorname{diag}\{\frac{1}{\sigma_{s,k}^2}\boldsymbol{w}\boldsymbol{w}^H, -\frac{2^{\bar{R}}}{\sigma_{e,l}^2}\boldsymbol{w}\boldsymbol{w}^H\}$, and $\hat{\boldsymbol{h}}_{k,l} = \begin{bmatrix} \hat{\boldsymbol{h}}_{s,k}^T & \hat{\boldsymbol{h}}_{e,l}^T \end{bmatrix}^T$.

Defining $\tilde{\boldsymbol{h}}_{k,l} \triangleq [\tilde{\boldsymbol{h}}_{s,k}^H\ \tilde{\boldsymbol{h}}_{e,l}^H]^H$, the outage constraint (5b) can be recast as

$$\begin{aligned}
\Pr\Big\{ &\tilde{\boldsymbol{h}}_{k,l}^H \operatorname{diag}\{\tfrac{1}{\sigma_s^2}\mathbf{E}_{s,k}^{\frac{1}{2}} \boldsymbol{w}\boldsymbol{w}^H \mathbf{E}_{s,k}^{\frac{1}{2}}, -\tfrac{2^{\bar{R}}}{\sigma_e^2}\mathbf{E}_{e,l}^{\frac{1}{2}} \boldsymbol{w}\boldsymbol{w}^H \mathbf{E}_{e,l}^{\frac{1}{2}}\} \tilde{\boldsymbol{h}}_{k,l} \\
&+ \operatorname{diag}\{\tfrac{1}{\sigma_s^2}\mathbf{E}_{s,k}^{\frac{1}{2}} \boldsymbol{w}\boldsymbol{w}^H, -\tfrac{2^{\bar{R}}}{\sigma_e^2}\mathbf{E}_{e,l}^{\frac{1}{2}} \boldsymbol{w}\boldsymbol{w}^H\} \hat{\boldsymbol{h}}_{k,l} - 2^{\bar{R}} \\
&+ \hat{\boldsymbol{h}}_{k,l}^H \bar{\mathbf{W}} \hat{\boldsymbol{h}}_{k,l} + 1 \ge 0 \Big\} \ge 1 - \rho_{k,l},\ \forall k, l,
\end{aligned} \tag{22}$$

which can be equivalently given as

$$\Pr\{\tilde{\boldsymbol{h}}_{k,l}^H \mathbf{C}_{k,l} \tilde{\boldsymbol{h}}_{k,l} + \tilde{\boldsymbol{h}}_{k,l}^H \boldsymbol{c}_{k,l} \le e_{k,l}\} \le \rho_{k,l},\ \forall k, l, \tag{23}$$

where $\mathbf{C}_{k,l} \triangleq \operatorname{diag}\{\frac{1}{\sigma_{s,k}^2}\mathbf{E}_{s,k}^{\frac{1}{2}} \boldsymbol{w}\boldsymbol{w}^H \mathbf{E}_{s,k}^{\frac{1}{2}}, -\frac{2^{\bar{R}}}{\sigma_{e,l}^2}\mathbf{E}_{e,l}^{\frac{1}{2}} \boldsymbol{w}\boldsymbol{w}^H \mathbf{E}_{e,l}^{\frac{1}{2}}\}$, $\boldsymbol{c}_{k,l} \triangleq \operatorname{diag}\{\frac{1}{\sigma_{s,k}^2}\mathbf{E}_{s,k}^{\frac{1}{2}} \boldsymbol{w}\boldsymbol{w}^H, -\frac{2^{\bar{R}}}{\sigma_{e,l}^2}\mathbf{E}_{e,l}^{\frac{1}{2}} \boldsymbol{w}\boldsymbol{w}^H\}\hat{\boldsymbol{h}}_{k,l}$, and $e_{k,l} \triangleq 2^{\bar{R}} - \hat{\boldsymbol{h}}_{k,l}^H \bar{\mathbf{W}} \hat{\boldsymbol{h}}_{k,l} - 1$.

Applying Lemma 1 and defining $\{x_{k,l}\}$ and $\{y_{k,l}\}$ as slack variables, the outage constraint (23) can be changed to the deterministic form (24) on the bottom of next page.

By introducing a variable $r_{k,l}$, the first constraint (24a) can be rewritten as

$$r_{k,l} \ge \frac{2^{\bar{R}}}{\sigma_{e,l}^2} \boldsymbol{w}^H (\hat{\boldsymbol{h}}_{e,l}\hat{\boldsymbol{h}}_{e,l}^H + \mathbf{E}_{e,l})\boldsymbol{w} + d_{k,l}, \tag{25a}$$

$$\frac{1}{\sigma_{s,k}^2} \boldsymbol{w}^H (\hat{\boldsymbol{h}}_{s,k}\hat{\boldsymbol{h}}_{s,k}^H + \mathbf{E}_{s,k})\boldsymbol{w} \ge r_{k,l}, \tag{25b}$$

where $d_{k,l} = \sqrt{-2\ln\rho_{k,l}}\, x_{k,l} - y_{k,l}\ln\rho_{k,l} + 2^{\bar{R}} - 1$. Adopting a similar method with (10b), the SCA method is employed to transform the concave constraint (25b) into the following linear constraint

$$\begin{aligned}
&\frac{1}{\sigma_{s,k}^2}\boldsymbol{w}^H(\hat{\boldsymbol{h}}_{s,k}\hat{\boldsymbol{h}}_{s,k}^H+\mathbf{E}_{s,k})\boldsymbol{w}\\
&\quad=\frac{1}{\sigma_{s,k}^2}(\boldsymbol{w}_0+\Delta\boldsymbol{w})^H(\hat{\boldsymbol{h}}_{s,k}\hat{\boldsymbol{h}}_{s,k}^H+\mathbf{E}_{s,k})(\boldsymbol{w}_0+\Delta\boldsymbol{w})\\
&\quad\geq\frac{1}{\sigma_{s,k}^2}\boldsymbol{w}_0^H(\hat{\boldsymbol{h}}_{s,k}\hat{\boldsymbol{h}}_{s,k}^H+\mathbf{E}_{s,k})\boldsymbol{w}_0\\
&\qquad+2\Re\{\boldsymbol{w}_0^H(\hat{\boldsymbol{h}}_{s,k}\hat{\boldsymbol{h}}_{s,k}^H+\mathbf{E}_{s,k})\Delta\boldsymbol{w}\}\\
&\quad\geq r_{k,l},
\end{aligned}\tag{26}$$

where (26) is derived by removing the quadratic form $\Delta\boldsymbol{w}^H(\hat{\boldsymbol{h}}_{s,k}\hat{\boldsymbol{h}}_{s,k}^H+\mathbf{E}_{s,k})\Delta\boldsymbol{w}$.

Next, for the second constraint (24b), applying the Cauchy-Schwarz inequality, we can obtain its convex approximation (27) on the bottom of this page. Here, $\left\|\mathrm{diag}\left\{\boldsymbol{w}\boldsymbol{w}^H,\boldsymbol{w}\boldsymbol{w}^H\right\}\right\|_F$ can be expressed as

$$\begin{aligned}
&\left\|\mathrm{diag}\left\{\boldsymbol{w}\boldsymbol{w}^H,\boldsymbol{w}\boldsymbol{w}^H\right\}\right\|_F\\
&\quad=\sqrt{\mathrm{tr}\left(\mathrm{diag}\left\{\boldsymbol{w}\boldsymbol{w}^H,\boldsymbol{w}\boldsymbol{w}^H\right\}\mathrm{diag}\left\{\boldsymbol{w}\boldsymbol{w}^H,\boldsymbol{w}\boldsymbol{w}^H\right\}\right)}\\
&\quad=\sqrt{\mathrm{tr}\left(\mathrm{diag}\left\{\boldsymbol{w}\boldsymbol{w}^H\boldsymbol{w}\boldsymbol{w}^H,\boldsymbol{w}\boldsymbol{w}^H\boldsymbol{w}\boldsymbol{w}^H\right\}\right)}\\
&\quad=\sqrt{2\mathrm{tr}\left(\boldsymbol{w}\boldsymbol{w}^H\boldsymbol{w}\boldsymbol{w}^H\right)}\\
&\quad\leq\sqrt{2}\|\boldsymbol{w}\|^2.
\end{aligned}\tag{28}$$

Defining $\omega_{k,l}\triangleq\mathrm{tr}\left(\mathrm{diag}\left\{\mathbf{E}_{s,k},\mathbf{E}_{e,l}\right\}\right)$ and $b_{k,l}\triangleq\sqrt{\omega_{k,l}^2+2\omega_{k,l}\|\hat{\boldsymbol{h}}_{k,l}\|^2}$, a more tractable form of (24b) is obtained as $\sqrt{2}\|\boldsymbol{w}\|^2b_{k,l}\leq x_{k,l}$, and it follows

$$2^{\frac{1}{4}}\left\|\boldsymbol{w}\right\|b_{k,l}^{\frac{1}{2}}\leq x_{k,l}^{\frac{1}{2}}.\tag{29}$$

Also, we can observe that the last constraint (24c) is always valid.

Combining all the results in (22)-(29), problem (5a) at the $(q+1)$-th iteration can be reformed as

$$\begin{aligned}
&\min_{\boldsymbol{w},\{x_{k,l}\},\{y_{k,l}\},\{r_{k,l}\},\{n_u\},\{m_u\},\{a_u\},\{b_u\}} \quad \|\boldsymbol{w}\|\\
&\quad s.t.\quad (13a),\ (17d),\ (25a),\ (26),\ (29),\ \Delta\boldsymbol{w}=\boldsymbol{w}-\boldsymbol{w}_q.
\end{aligned}\tag{30}$$

Problem (30) is again an SOCP problem, which can be solved by CVX [44]. Therefore, the convergence property of this algorithm can be proved similarly to Theorem 1 and thus its proof is omitted.

V. Computational Complexity

In this section, we evaluate the computational complexity of the proposed robust design methods. As will be shown in Section VI, the SOCP-SCA algorithm exhibits gains in terms of both computational complexity and performance compared to the conventional SDP-GR algorithm and SDP-CCCP algorithm [48].

Now, we will present the complexity comparison by adopting the analysis in [31]. The complexities of all algorithms are shown in Table I on the top of next page. Here, we denote n, $L^{\max}$ and $Q^{\max}$ as the number of decision variables, the CCCP and SCA iteration number, respectively.

$$\frac{1}{\sigma_{s,k}^2}\boldsymbol{w}^H(\hat{\boldsymbol{h}}_{s,k}\hat{\boldsymbol{h}}_{s,k}^H+\mathbf{E}_{s,k})\boldsymbol{w}-\frac{2^{\bar{R}}}{\sigma_{e,l}^2}\boldsymbol{w}^H(\hat{\boldsymbol{h}}_{e,l}\hat{\boldsymbol{h}}_{e,l}^H+\mathbf{E}_{e,l})\boldsymbol{w}-\sqrt{-2\ln\rho_{k,l}}x_{k,l}+y_{k,l}\ln\rho_{k,l}\geq 2^{\bar{R}}-1,\tag{24a}$$

$$\sqrt{\left\|\mathrm{diag}\left\{\frac{1}{\sigma_{s,k}^2}\mathbf{E}_{s,k}^{\frac{1}{2}}\boldsymbol{w}\boldsymbol{w}^H\mathbf{E}_{s,k}^{\frac{1}{2}},-\frac{2^{\bar{R}}}{\sigma_{e,l}^2}\mathbf{E}_{e,l}^{\frac{1}{2}}\boldsymbol{w}\boldsymbol{w}^H\mathbf{E}_{e,l}^{\frac{1}{2}}\right\}\right\|_F^2+2\left\|\mathrm{diag}\left\{\frac{1}{\sigma_{s,k}^2}\mathbf{E}_{s,k}^{\frac{1}{2}}\boldsymbol{w}\boldsymbol{w}^H,-\frac{2^{\bar{R}}}{\sigma_{e,l}^2}\mathbf{E}_{e,l}^{\frac{1}{2}}\boldsymbol{w}\boldsymbol{w}^H\right\}\hat{\boldsymbol{h}}_{k,l}\right\|^2}\leq x_{k,l},\tag{24b}$$

$$y_{k,l}\mathbf{I}_{2M_{\mathrm{T}}}+\mathrm{diag}\left\{\frac{1}{\sigma_{s,k}^2}\mathbf{E}_{s,k}^{\frac{1}{2}}\boldsymbol{w}\boldsymbol{w}^H\mathbf{E}_{s,k}^{\frac{1}{2}},-\frac{2^{\bar{R}}}{\sigma_{e,l}^2}\mathbf{E}_{e,l}^{\frac{1}{2}}\boldsymbol{w}\boldsymbol{w}^H\mathbf{E}_{e,l}^{\frac{1}{2}}\right\}\succeq\mathbf{0},\ y_{k,l}\geq 0,\ \forall k,l,\tag{24c}$$

$$\begin{aligned}
&\sqrt{\left\|\mathrm{diag}\left\{\frac{1}{\sigma_{s,k}^2}\mathbf{E}_{s,k}^{\frac{1}{2}}\boldsymbol{w}\boldsymbol{w}^H\mathbf{E}_{s,k}^{\frac{1}{2}},-\frac{2^{\bar{R}}}{\sigma_{e,l}^2}\mathbf{E}_{e,l}^{\frac{1}{2}}\boldsymbol{w}\boldsymbol{w}^H\mathbf{E}_{e,l}^{\frac{1}{2}}\right\}\right\|_F^2+2\left\|\mathrm{diag}\left\{\frac{1}{\sigma_{s,k}^2}\mathbf{E}_{s,k}^{\frac{1}{2}}\boldsymbol{w}\boldsymbol{w}^H,-\frac{2^{\bar{R}}}{\sigma_{e,l}^2}\mathbf{E}_{e,l}^{\frac{1}{2}}\boldsymbol{w}\boldsymbol{w}^H\right\}\hat{\boldsymbol{h}}_{k,l}\right\|^2}\\
&\leq\sqrt{\left\|\mathrm{diag}\left\{\frac{1}{\sigma_{s,k}^2}\mathbf{E}_{s,k}^{\frac{1}{2}}\boldsymbol{w}\boldsymbol{w}^H,-\frac{2^{\bar{R}}}{\sigma_{e,l}^2}\mathbf{E}_{e,l}^{\frac{1}{2}}\boldsymbol{w}\boldsymbol{w}^H\right\}\right\|_F^2\left(\left\|\mathrm{diag}\left\{\frac{1}{\sigma_{s,k}^2}\mathbf{E}_{s,k}^{\frac{1}{2}},-\frac{2^{\bar{R}}}{\sigma_{e,l}^2}\mathbf{E}_{e,l}^{\frac{1}{2}}\right\}\right\|_F^2+2\left\|\hat{\boldsymbol{h}}_{k,l}\right\|^2\right)}\\
&\leq\sqrt{\left\|\mathrm{diag}\left\{\boldsymbol{w}\boldsymbol{w}^H,\boldsymbol{w}\boldsymbol{w}^H\right\}\right\|_F^2\left(\mathrm{tr}^2\left(\mathrm{diag}\left\{\frac{1}{\sigma_{s,k}^2}\mathbf{E}_{s,k},-\frac{2^{\bar{R}}}{\sigma_{e,l}^2}\mathbf{E}_{e,l}\right\}\right)+2\mathrm{tr}\left(\mathrm{diag}\left\{\frac{1}{\sigma_{s,k}^2}\mathbf{E}_{s,k},-\frac{2^{\bar{R}}}{\sigma_{e,l}^2}\mathbf{E}_{e,l}\right\}\right)\left\|\hat{\boldsymbol{h}}_{k,l}\right\|^2\right)}\\
&=\left\|\mathrm{diag}\left\{\boldsymbol{w}\boldsymbol{w}^H,\boldsymbol{w}\boldsymbol{w}^H\right\}\right\|_F\sqrt{\mathrm{tr}^2\left(\mathrm{diag}\left\{\frac{1}{\sigma_{s,k}^2}\mathbf{E}_{s,k},-\frac{2^{\bar{R}}}{\sigma_{e,l}^2}\mathbf{E}_{e,l}\right\}\right)+2\mathrm{tr}\left(\mathrm{diag}\left\{\frac{1}{\sigma_{s,k}^2}\mathbf{E}_{s,k},-\frac{2^{\bar{R}}}{\sigma_{e,l}^2}\mathbf{E}_{e,l}\right\}\right)\left\|\hat{\boldsymbol{h}}_{k,l}\right\|^2}\leq x_{k,l}.
\end{aligned}\tag{27}$$

TABLE I

COMPLEXITY ANALYSIS OF DIFFERENT ALGORITHMS

Algorithms		Complexity Order
PCU	SOCP-SCA	$\mathcal{O}\big(nQ^{max}\sqrt{6KL+4L+6U}\big[(2KL+2L+2U)(M_{\mathrm{T}}+1)^2+2KL+2U+n^2\big]\big)$ where $n=\mathcal{O}(M_{\mathrm{T}}+3KL+2L+4U)$
	SDP-GR	$\mathcal{O}\big(n\sqrt{KLM_{\mathrm{T}}+UM_{\mathrm{T}}+4KL+4U+M_{\mathrm{T}}}\big[(KL+U+1)M_{\mathrm{T}}^3+n((KL+U+1)M_{\mathrm{T}}^2+2KL+3)+(KL+1)(M_{\mathrm{T}}^2+M_{\mathrm{T}}+1)+2KL+2+n^2\big]\big)$ where $n=\mathcal{O}(M_{\mathrm{T}}^2+2KL+2U)$
	SDP-CCCP	$\mathcal{O}\big(nL^{max}\sqrt{(KL+U+2)M_{\mathrm{T}}+4KL+4U+2}\big[(KL+U+1)M_{\mathrm{T}}^3+(2M_{\mathrm{T}}+1)^3+n((KL+U+1)M_{\mathrm{T}}^2+(2M_{\mathrm{T}}+1)^2+2KL+2U+1)+(KL+U)(M_{\mathrm{T}}^2+M_{\mathrm{T}}+1)+2KL+2U+1+n^2\big]\big)$ where $n=\mathcal{O}(3M_{\mathrm{T}}^2+M_{\mathrm{T}}+2KL+2U)$
FCU	SOCP-SCA	$\mathcal{O}\big(nQ^{max}\sqrt{5KL+6U}[(2KL+2U)(M_{\mathrm{T}}+1)^2+KL+2U+n^2]\big)$ where $n=\mathcal{O}(M_{\mathrm{T}}+3KL+4U)$
	SDP-GR	$\mathcal{O}\big(n\sqrt{(2KL+U)M_{\mathrm{T}}+4KL+4U}\big[8KLM_{\mathrm{T}}^3+(U+1)M_{\mathrm{T}}^3+n(4KLM_{\mathrm{T}}^2+2M_{\mathrm{T}}^2+2KL+2U)+KL(2M_{\mathrm{T}}^2+2M_{\mathrm{T}}+1)+U(M_{\mathrm{T}}^2+M_{\mathrm{T}}+1)+2KL+2U+n^2\big]\big)$ where $n=\mathcal{O}(M_{\mathrm{T}}^2+2KL+2U)$
	SDP-CCCP	$\mathcal{O}\big(nL^{max}\sqrt{(2KL+U+3)M_{\mathrm{T}}+4U+4KL+2}[8KLM_{\mathrm{T}}^3+(U+1)M_{\mathrm{T}}^3+(2M_{\mathrm{T}}+1)^3+n(4KLM_{\mathrm{T}}^2+(U+1)M_{\mathrm{T}}^2+(2M_{\mathrm{T}}+1)^2+2KL+2U+1)+KL(2M_{\mathrm{T}}^2+M_{\mathrm{T}}+1)+(M_{\mathrm{T}}^2+M_{\mathrm{T}}+1)+2KL+2U+1+n^2]\big)$ where $n=\mathcal{O}(3M_{\mathrm{T}}^2+M_{\mathrm{T}}+2KL+2U)$

1) SOCP-SCA for PCU in problem (20) involves $2KL+2L+2U$ SOCs of dimension $M_{\mathrm{T}}+1$ and $2KL+2U$ linear constraints.

2) SDP-GR for PCU has $KL+U$ SOCs constraints of dimension $M_{\mathrm{T}}^2+M_{\mathrm{T}}+1$, $KL+U+1$ LMI constraints of size M_{T}, and $2KL+2U$ linear constraints.

3) SDP-CCCP for PCU consists of $KL+U$ SOCs constraints of dimension $M_{\mathrm{T}}^2+M_{\mathrm{T}}+1$, $KL+U$ LMI constraints of size M_{T}, one LMI constraint of size $2M_{\mathrm{T}}+1$, and $2KL+2U+1$ linear constraints.

4) SOCP-SCA for FCU in problem (30) involves $2KL+2U$ SOCs of dimension $M_{\mathrm{T}}+1$ and $KL+2U$ linear constraints.

5) SDP-GR for FCU contains KL SOCs constraints of dimension $2M_{\mathrm{T}}^2+2M_{\mathrm{T}}+1$, U SOC constraint of dimension $M_{\mathrm{T}}^2+M_{\mathrm{T}}+1$, KL LMI constraints of size $2M_{\mathrm{T}}$, $U+1$ LMI constraints of size M_{T}, and $2KL+2U$ linear constraints.

6) SDP-CCCP for FCU is made up of KL SOCs constraints of dimension $2M_{\mathrm{T}}^2+2M_{\mathrm{T}}+1$, U SOC constraint of dimension $M_{\mathrm{T}}^2+M_{\mathrm{T}}+1$, KL LMI constraints of size $2M_{\mathrm{T}}$, $U+1$ LMI constraints of size M_{T}, one LMI constraint of size $2M_{\mathrm{T}}+2U+1$, and $2KL+3$ linear constraints.

For example, for a system with $K=2, L=2$, $U=2$, $M_{\mathrm{T}}=5$, and $L^{\max}=Q^{\max}=10$, the complexities of the SOCP-SCA, SDP-GR and SDP-CCCP algorithms for the PCU case are $\mathcal{O}(2.42\times10^6)$, $\mathcal{O}(2.64\times10^6)$ and $\mathcal{O}(2.94\times10^8)$, respectively, while those for the FCU case are $\mathcal{O}(1.50\times10^6)$, $\mathcal{O}(7.37\times10^7)$ and $\mathcal{O}(6.08\times10^8)$, respectively.

VI. SIMULATION RESULTS

In this section, we provide the simulation results to validate the performance of our proposed algorithms. We consider a system with two legitimate users, two eavesdroppers and two EH receivers. The transmitter is equipped with six transmit antennas ($M_{\mathrm{T}}=6$). We assume the channel models with both large-scale and small-scale fading. The simplified large-scale fading model is expressed as $D=\left(\frac{d}{d_0}\right)^{-\alpha}$, where d represents the distance between the transmitter and the receiver, d_0 is the reference distance set to be 1 m, and $\alpha=3$ equals the path loss exponent [45]. We define $d_s=12$ m as the distance between the transmitter and the legitimate users, $d_e=6$ m as the distance between the transmitter and the eavesdroppers, and $d_h=4$ m as the distance between the transmitter and the EH receiver as in [23], unless specified otherwise. All channel coefficients are modelled as Rician fading. The channel vector $\boldsymbol{h}_{s,k}$ is given as $\boldsymbol{h}_{s,k}=\sqrt{\frac{K_R}{1+K_R}}\boldsymbol{h}_{s,k}^{LOS}+\sqrt{\frac{1}{1+K_R}}\boldsymbol{h}_{s,k}^{NLOS}$, where $\boldsymbol{h}_{s,k}^{LOS}$ indicates the line-of-sight (LOS) component with $\|\boldsymbol{h}_{s,k}^{LOS}\|^2=D$, $\boldsymbol{h}_{s,k}^{NLOS}$ represents the Rayleigh fading component as $\boldsymbol{h}_{s,k}^{NLOS}\sim\mathcal{CN}(0,D\mathbf{I})$, and K_R is the Rician factor equal to 3. For the LOS component, we apply the far-field uniform linear antenna array to model the channels in [46]. For simplicity, it is assumed that $\sigma_{s,k}^2=\sigma_s^2=-60$ dBm and $\sigma_{e,l}^2=\sigma_e^2=-60$ dBm for $\forall l,k$. In addition, we define the outage probability as $\rho_{k,l}=0.05, \forall k,l$, and $\rho_e=0.05$, and the channel error covariance matrix as $\mathbf{E}_{s,k}=\mathbf{E}_s=\varepsilon_s^2\mathbf{I}$, $\mathbf{E}_{e,l}=\mathbf{E}_e=\varepsilon_e^2\mathbf{I}$, and $\mathbf{E}_{h,u}=\varepsilon_h^2\mathbf{I}$ for $\forall k,l,u$. In our simulations, we compare the following transmit designs: the SDP-GR algorithm, the SDP-CCCP algorithm, the proposed SOCP-SCA algorithm, and the perfect CSI case where the channel error is set to zero.

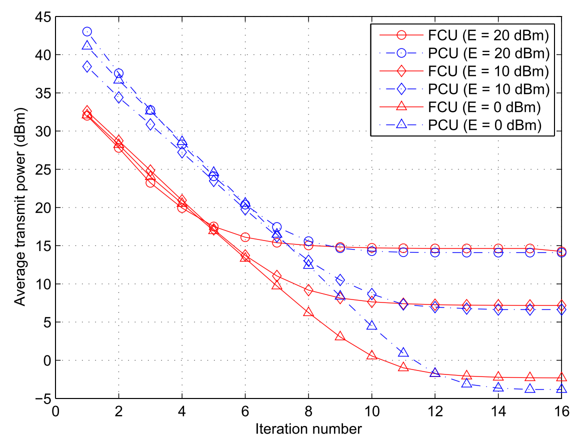

Fig. 1. Average transmit power w.r.t. iteration numbers for the SOCP-SCA algorithm with various E.

Fig. 1 illustrates the convergence performance of the SOCP-SCA algorithm with respect to iteration numbers. Here, we set $\bar{E}=E$, $\bar{R}=1$ bps/Hz, and $\varepsilon_s=\varepsilon_e=\varepsilon_h=0.01$. It is easily seen from the plots that the convergence of all cases can be quickly achieved within 14 iterations, and the convergence speed becomes fast as E increases. It is observed that the PCU schemes converges slower than the FCU schemes for the SOCP-SCA regardless of E. This is due to the fact that

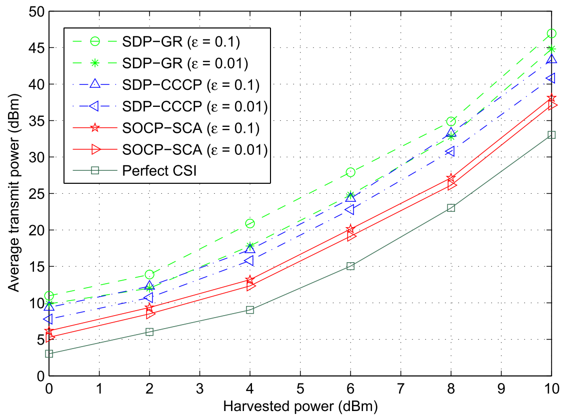

Fig. 2. Average transmit power with respect to the harvested power for FCU.

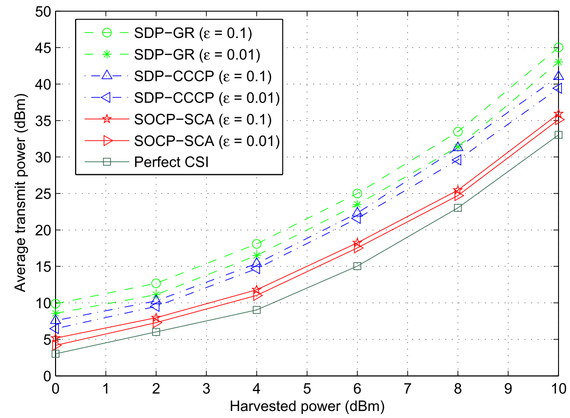

Fig. 4. Average transmit power with respect to the harvested power for PCU.

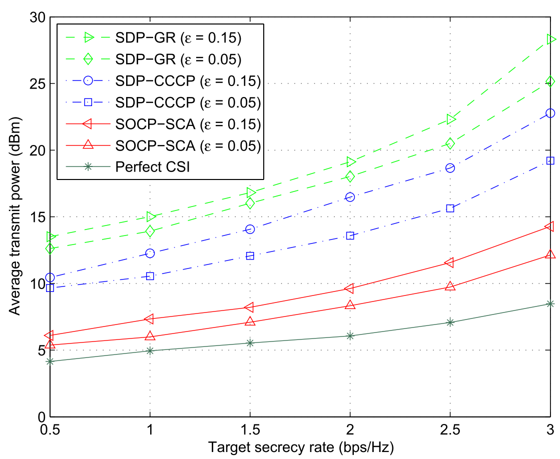

Fig. 3. Average transmit power with respect to the target secrecy rate for FCU.

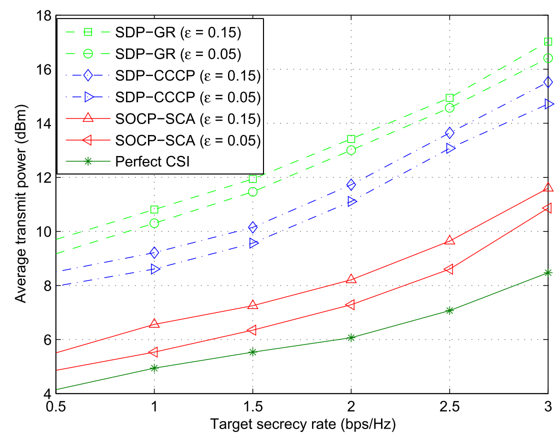

Fig. 5. Average transmit power with respect to the target secrecy rate for PCU.

the number of variables in the PCU scheme is greater than the FCU scheme for the SOCP-SCA algorithm.

For the FCU case, we present the performance of all robust algorithms in terms of the average transmit power in Figures 2 and 3. Fig. 2 evaluates the performance among the proposed robust algorithms with $\bar{R} = 0.5$ bps/Hz by averaging the transmit power over 500 feasible channel realizations. We can check that the proposed SOCP-SCA algorithm requires lower average transmit power than the conventional SDP-GR and SDP-CCCP algorithms. Performance gains of the SOCP-SCA algorithm with $\varepsilon = 0.01$ and 0.1 over the SDP-GR algorithm are 6.1 dB and 8.2 dB, respectively, while those over the SDP-CCCP algorithm are 5.1 dB and 4.3 dB, respectively.

Fig. 3 compares the average transmit power with respect to the target secrecy rate with $E = 3$ dBm. It is observed that the transmit power for the perfect CSI scheme grows slower than all the robust schemes as $\bar{R}$ increases. We can see that for $\varepsilon = 0.05$ and 0.15, the SOCP-SCA algorithm outperforms the SDP-GR and the SDP-CCCP algorithms. Also, a performance gain of the SOCP-SCA algorithm over the SDP-GR and SDP-CCCP grows as $\bar{R}$ increases. For $\varepsilon = 0.15$, the performance gap between the SOCP-SCA and the conventional algorithms becomes large at high secrecy rate region. This is because higher-rank solutions may be returned in the SDP-GR algorithm.

For the PCU case, the transmit power performance is plotted in Fig. 4 with $\bar{R} = 0.5$ bps/Hz. One can observe from Fig. 4 that the average transmit power increases as the harvested power becomes large. Also, the performance gains of SOCP-SCA algorithm with $\varepsilon = 0.01$ and 0.1 over the SDP-GR algorithm are 6.1 dB and 7.2 dB at all harvested power region, respectively, while those over the SDP-CCCP algorithm are 3.8 dB and 4.1 dB, respectively.

Also, in Fig. 5, the transmit power is illustrated with $E = 2$ dBm. We can see that the SOCP-SCA algorithm with $\varepsilon = 0.05$ outperforms the SDP-CCCP algorithm by 4.3 dB, and the performance gains of the SOCP-SCA over the SDP-GR algorithm become larger as the target secrecy rate increase. Similarly, for the $\varepsilon = 0.15$ case, the performance gap between the SOCP-SCA and the SDP-GR algorithms grows at high secrecy rate region.

Fig. 6 compares the average central processing unit (CPU) execution time of the proposed algorithms and the conventional schemes for a given channel realization with various M_{T} on a personal computer.[1] Here, we set that $\bar{R} = 1$ bps/Hz and $E = 20$ dBm. It is observed that the SOCP-SCA algorithm requires shorter CPU running time than the conventional scheme at all M_{T} region. Also, the difference in the execution time between the SOCP-SCA and

[1] All the modelling and solutions of the algorithms are performed using the CVX tool [44] on a desktop Intel Core i7-4700HQ CPU running at 2.4 GHz with 4 GB RAM. The version of Matlab is R2010a.

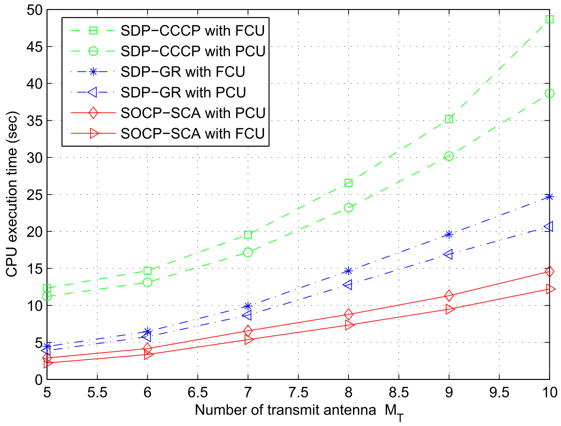

Fig. 6. Average CPU execution time with respect to the number of transmit antennas.

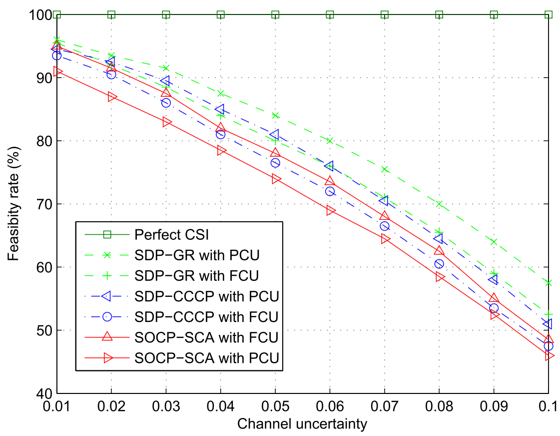

Fig. 7. Feasibility rate with respect to channel uncertainties.

conventional algorithm becomes big as M_{T} increases. For example, with $M_T = 8$, the running time of the SOCP-SCA is only 59.6% and 32.7% of the SDP-GR and SDP-CCCP, respectively.

Finally, we present the feasibility rates of all design schemes in Fig. 7, where the simulation results are obtained over 1000 channel realizations with $\rho_{k,l} = \rho_e = 0.05$, $\bar{R} = 0.5$ bps/Hz and $E = 5$ dBm. In this plot, one can see that the feasibility rate of the SOCP-SCA algorithm is higher than that of the SDP-CCCP scheme for FCU. This is due to the introduction of less variables compared to the conventional SDP-CCCP scheme. With the increase of channel uncertainties, the feasibility rate of all schemes decline.

VII. Conclusion

In this paper, we have studied robust secure beamforming designs for secure broadcasting channels in MISO SWIPT systems under different statistical channel uncertainty models. Our aim is to minimize the transmit power subject to the secrecy rate outage probability constraint and the harvested energy outage probability constraint. In order to obtain a rank-one solution, we have proposed an SOCP-SCA robust design scheme with low-complexity for partial channel uncertainty case. Moreover, we have extended the proposed algorithm to the full channel uncertainty model. Finally, simulation results have shown that the proposed robust designs outperforms the conventional scheme with reduced complexity.

Appendix
Proof of Theorem 1

The convergence result of Algorithm 1 has been studied in [47], which is briefly presented here for the sake of completeness. From (10)-(13), we have the following inequalities for the $(q+1)$-th iteration.

$$\begin{aligned}
&\frac{2^{-\bar{R}}\sigma_{e,l}^2}{\sigma_{s,k}^2}\boldsymbol{w}^H\boldsymbol{h}_{s,k}\boldsymbol{h}_{s,k}^H\boldsymbol{w}\\
&\quad\geq \frac{2^{-\bar{R}}\sigma_{e,l}^2}{\sigma_{s,k}^2}(\boldsymbol{w}_q^{*H}\boldsymbol{h}_{s,k}\boldsymbol{h}_{s,k}^H\boldsymbol{w}_q^* + 2\Re\{\boldsymbol{w}_q^{*H}\boldsymbol{h}_{s,k}\boldsymbol{h}_{s,k}^H\Delta\boldsymbol{w}\})\\
&\quad\geq t_{k,l}, \qquad (31a)\\
&\boldsymbol{w}^H(\mathbf{E}_{h,u}+\hat{\boldsymbol{h}}_{h,u}\hat{\boldsymbol{h}}_{h,u}^H)\boldsymbol{w}\\
&\quad\geq \boldsymbol{w}_q^{*H}(\mathbf{E}_{h,u}+\hat{\boldsymbol{h}}_{h,u}\hat{\boldsymbol{h}}_{h,u}^H)\boldsymbol{w}_q^*\\
&\qquad + 2\Re\{\boldsymbol{w}_q^{*H}(\mathbf{E}_{h,u}+\hat{\boldsymbol{h}}_{h,u}\hat{\boldsymbol{h}}_{h,u}^H)\Delta\boldsymbol{w}\}\\
&\quad\geq \sqrt{-2\ln\rho_u}m - n\ln\rho_u + \bar{E}, \qquad (31b)
\end{aligned}$$

which are conservative convex approximations with $\boldsymbol{w}_{q+1}^* = \boldsymbol{w}_q^* + \Delta\boldsymbol{w}$.

Due to the linear approximations adopted in (31), the updating rule in Algorithm 1 ensures that $\boldsymbol{w}_q^*$ is feasible to the optimization problem at the $(q+1)$-th iteration. Thus, it immediately holds that $f_{q+1}^*(\boldsymbol{w}_{q+1}^*) \leq f_q^*(\boldsymbol{w}_q^*)$. In other words, Algorithm 1 yields a non-increasing sequence of objective values. Because of the secrecy rate constraint and harvested energy constraint, problem (20) is bounded, and thus Algorithm 1 is guaranteed to converge to some local optimum solution, i.e., $\|\Delta\boldsymbol{w}\| = 0$ and $f_q^*(\boldsymbol{w}_q^*) = f_{q+1}^*(\boldsymbol{w}_{q+1}^*)$. ■

References

[1] V. Raghunathan, S. Ganeriwal, and M. Srivastava, "Emerging techniques for long lived wireless sensor networks," *IEEE Commun. Mag.*, vol. 44, no. 4, pp. 108–114, Apr. 2006.

[2] E. Hossain, M. Rasti, H. Tabassum, and A. Abdelnasser, "Evolution toward 5G multi-tier cellular wireless networks: An interference management perspective," *IEEE Wireless Commun.*, vol. 21, no. 3, pp. 118–127, Jun. 2014.

[3] Z. Ding *et al.*, "Application of smart antenna technologies in simultaneous wireless information and power transfer," *IEEE Commun. Mag.*, vol. 53, no. 4, pp. 86–93, Apr. 2015.

[4] L. Mohjazi, M. Dianati, G. K. Karagiannidis, S. Muhaidat, and M. Al-Qutayri, "RF-powered cognitive radio networks: Technical challenges and limitations," *IEEE Commun. Mag.*, vol. 53, no. 4, pp. 94–100, Apr. 2015.

[5] Z. Zhu, Z. Chu, Z. Wang, and I. Lee, "Joint optimization of AN-aided beamforming and power splitting designs for MISO secrecy channel with SWIPT," in *Proc. IEEE ICC*, May 2016, pp. 1–6.

[6] D. W. K. Ng, E. S. Lo, and R. Schober, "Energy-efficient resource allocation in OFDMA systems with hybrid energy harvesting base station," *IEEE Trans. Wireless Commun.*, vol. 12, no. 7, pp. 3412–3427, Jul. 2013.

[7] S. Bi, C. K. Ho, and R. Zhang, "Wireless powered communication: Opportunities and challenges," *IEEE Commun. Mag.*, vol. 53, no. 4, pp. 117–125, Apr. 2015.

[8] J. Zhang, B. Zhang, S. Chen, X. Mu, M. El-Hajjar, and L. Hanzo, "Pilot contamination elimination for large-scale multiple-antenna aided OFDM systems," *IEEE J. Sel. Topics Signal Process.*, vol. 8, no. 5, pp. 759–772, Oct. 2014.

[9] Z. Zhu, Z. Wang, Z. Chu, X. Gao, Y. Zhang, and J. Cui, "Robust beamforming based on transmit power analysis for multiuser multiple-input–single-output interference channels with energy harvesting," *IET Commun.*, vol. 10, no. 10, pp. 1221–1228, Jul. 2016.

[10] Z. Zhu, K.-J. Lee, Z. Wang, and I. Lee, "Robust beamforming and power splitting design in distributed antenna system with SWIPT under bounded channel uncertainty," in *Proc. IEEE VTC Spring*, May 2015, pp. 1–5.

[11] Z. Zhu, Z. Wang, K. J. Lee, Z. Chu, and I. Lee, "Robust transceiver designs in multiuser MISO broadcasting with simultaneous wireless information and power transmission," *J. Commun. Netw.*, vol. 18, no. 2, pp. 173–181, Apr. 2016.

[12] H. Lee, S.-R. Lee, K.-J. Lee, and I. Lee, "Optimal beamforming designs for wireless information and power transfer in MISO interference channels," *IEEE Trans. Wireless Commun.*, vol. 14, no. 9, pp. 4810–4821, Sep. 2015.

[13] J. Xu, L. Liu, and R. Zhang, "Multiuser MISO beamforming for simultaneous wireless information and power transfer," *IEEE Trans. Signal Process.*, vol. 62, no. 18, pp. 4798–4810, Sep. 2014.

[14] X. Gui, Z. Zhu, and I. Lee, "Sum rate maximizing in a multi-user MIMO system with SWIPT," in *Proc. IEEE VTC Spring,* May 2015, pp. 1–5.

[15] Z. Chu, K. Cumanan, Z. Ding, M. Johnston, and S. Y. Le Goff, "Secrecy rate optimizations for a MIMO secrecy channel with a cooperative jammer," *IEEE Trans. Veh. Technol.*, vol. 64, no. 5, pp. 1833–1847, May 2015.

[16] Z. Chu, K. Cumanan, Z. Ding, M. Johnston, and S. L. Goff, "Robust outage secrecy rate optimizations for a MIMO secrecy channel," *IEEE Wireless Commun. Lett.*, vol. 4, no. 1, pp. 86–89, Feb. 2015.

[17] Z. Zhu, K.-J. Lee, Z. Wang, Z. Chu, and I. Lee, "Robust precoding methods for multiuser MISO wireless energy harvesting systems," in *Proc. IEEE VTC Fall*, Sep. 2015, pp. 1–5.

[18] Z. Chu, Z. Zhu, and J. Hussein, "Robust optimization for AN-aided transmission and power splitting for secure MISO SWIPT system," *IEEE Commun. Lett.*, vol. 20, no. 8, pp. 1571–1574, Aug. 2016.

[19] L. Liu, R. Zhang, and K.-C. Chua, "Secrecy wireless information and power transfer with MISO beamforming," *IEEE Trans. Signal Process.*, vol. 62, no. 7, pp. 1850–1863, Apr. 2014.

[20] Q. Li, Q. Zhang, and J. Qin, "Secure relay beamforming for simultaneous wireless information and power transfer in nonregenerative relay networks," *IEEE Trans. Veh. Technol.*, vol. 63, no. 5, pp. 2462–2467, Jun. 2014.

[21] H. Xing, Z. Chu, Z. Ding, and A. Nallanathan, "Harvest-and-jam: Improving security for wireless energy harvesting cooperative networks," in *Proc. IEEE Globecom*, Dec. 2014, pp. 3145–3150.

[22] Q. Shi, W. Xu, J. Wu, E. Song, and Y. Wang, "Secure beamforming for MIMO broadcasting with wireless information and power transfer," *IEEE Trans. Wireless Commun.*, vol. 14, no. 5, pp. 2841–2853, May 2015.

[23] H. Xing, L. Liu, and R. Zhang, "Secrecy wireless information and power transfer in fading wiretap channel," *IEEE Trans. Veh. Technol.*, vol. 65, no. 1, pp. 180–190, Jan. 2016.

[24] D. W. K. Ng and R. Schober, "Secure and green SWIPT in distributed antenna networks with limited backhaul capacity," *IEEE Trans. Wireless Commun.*, vol. 14, no. 9, pp. 5082–5097, Sep. 2015.

[25] D. W. K. Ng, E. S. Lo, and R. Schober, "Robust beamforming for secure communication in systems with wireless information and power transfer," *IEEE Trans. Wireless Commun.*, vol. 13, no. 8, pp. 4599–4615, Aug. 2014.

[26] M. R. A. Khandaker and K.-K. Wong, "Robust secrecy beamforming with energy-harvesting eavesdroppers," *IEEE Wireless Commun. Lett.*, vol. 4, no. 1, pp. 10–13, Feb. 2015.

[27] M. R. A. Khandaker and K.-K. Wong, "Masked beamforming in the presence of energy-harvesting eavesdroppers," *IEEE Trans. Inf. Forensics Security*, vol. 10, no. 1, pp. 40–54, Jan. 2015.

[28] R. Feng, Q. Li, Q. Zhang, and J. Qin, "Robust secure transmission in MISO simultaneous wireless information and power transfer system," *IEEE Trans. Veh. Technol.*, vol. 64, no. 1, pp. 400–405, Jan. 2015.

[29] M. Tian, X. Huang, Q. Zhang, and J. Qin, "Robust AN-aided secure transmission scheme in MISO channels with simultaneous wireless information and power transfer," *IEEE Signal Process. Lett.*, vol. 22, no. 6, pp. 723–727, Jun. 2015.

[30] Q. Zhang, X. Huang, Q. Li, and J. Qin, "Cooperative jamming aided robust secure transmission for wireless information and power transfer in MISO channels," *IEEE Trans. Commun.*, vol. 63, no. 3, pp. 906–915, Mar. 2015.

[31] K.-Y. Wang, A. M.-C. So, T.-H. Chang, W.-K. Ma, and C.-Y. Chi, "Outage constrained robust transmit optimization for multiuser MISO downlinks: Tractable approximations by conic optimization," *IEEE Trans. Signal Process.*, vol. 62, no. 21, pp. 5690–5705, Nov. 2014.

[32] S. Ma, M. Hong, E. Song, X. Wang, and D. Sun, "Outage constrained robust secure transmission for MISO wiretap channels," *IEEE Trans. Wireless Commun.*, vol. 13, no. 10, pp. 5558–5570, Oct. 2014.

[33] Z. Chu, H. Xing, M. Johnston, and S. Le Goff, "Secrecy rate optimizations for a MISO secrecy channel with multiple multiantenna eavesdroppers," *IEEE Trans. Wireless Commun.*, vol. 15, no. 1, pp. 283–297, Jan. 2016.

[34] Z.-Q. Luo, W.-K. Ma, A.-C. So, Y. Ye, and S. Zhang, "Semidefinite relaxation of quadratic optimization problems," *IEEE Trans. Signal Process. Mag.*, vol. 27, no. 3, pp. 20–34, May 2010.

[35] W. Xu, A. Tajer, X. Wang, and S. Alshomrani, "Power Allocation in MISO Interference Channels with Stochastic CSIT," *IEEE Trans. Wireless Commun.*, vol. 13, no. 3, pp. 1716–1727, Mar. 2014.

[36] U. Rashid, H. D. Tuan, H. H. Kha, and H. H. Nguyen, "Joint optimization of source precoding and relay beamforming in wireless MIMO relay networks," *IEEE Trans. Commun.*, vol. 62, no. 2, pp. 488–499, Feb. 2014.

[37] J. Xiao, C. Xu, Q. Zhang, X. Huang, and J. Qin, "Robust transceiver design for two-user MIMO interference channel with simultaneous wireless information and power transfer," *IEEE Trans. Veh. Technol.*, vol. 65, no. 5, pp. 3823–3828, May 2016.

[38] M. Razaviyayn, M. Hong, and Z.-Q. Luo, "A unified convergence analysis of block successive minimization methods for nonsmooth optimization," *SIAM J. Optim.*, vol. 23, no. 2, pp. 1126–1153, 2013.

[39] W.-C. Li, T.-H. Chang, C. Lin, and C.-Y. Chi, "Coordinated beamforming for multiuser MISO interference channel under rate outage constraints," *IEEE Trans. Signal Process.*, vol. 61, no. 5, pp. 1087–1103, Mar. 2013.

[40] D. Li, C. Shen, and Z. Qiu, "Sum rate maximization and energy harvesting for two-way AF relay systems with imperfect CSI," in *Proc. IEEE ICASSP*, May 2013, pp. 4958–4962.

[41] Z. Chu, Z. Zhu, M. Johnston, and S. Le Goff, "Simultaneous wireless information power transfer for MISO secrecy channel," *IEEE Trans. Veh. Technol*, to be published.

[42] M. S. Lobo, L. Vandenberghe, S. Boyd, and H. Lebret, "Applications of second-order cone programming," *Linear Algebra Appl.*, vol. 284, nos. 1–3, pp. 193–228, 1998.

[43] S. Boyd and L. Vandenberghe, *Convex Optimization*. Cambridge, U.K.: Cambridge Univ. Press, 2004.

[44] M. Grant and S. Boyd. (Sep. 2012). *CVX: MATLAB Software for Disciplined Convex Programming*. [Online]. Available: http://cvxr.com/cvx

[45] H. Wang, S. Ma, T.-S. Ng, and H. V. Poor, "A general analytical approach for opportunistic cooperative systems with spatially random relays," *IEEE Trans. Wireless Commun.*, vol. 10, no. 12, pp. 4122–4129, Dec. 2011.

[46] E. Karipidis, N. D. Sidiropoulos, and Z. Q. Luo, "Far-field multicast beamforming for uniform linear antenna arrays," *IEEE Trans. Signal Process.*, vol. 55, no. 10, pp. 4916–4927, Oct. 2007.

[47] A. Beck, A. Ben-Tal, and L. Tetruashvili, "A sequential parametric convex approximation method with applications to nonconvex truss topology design problems," *J. Global Optim.*, vol. 47, no. 1, pp. 29–51, May 2010.

[48] Z. Zhu, Z. Chu, Z. Wang, and I. Lee, "Robust beamforming design for MISO secrecy multicasting systems with energy harvesting," in *Proc. IEEE VTC Spring*, May 2016, pp. 1–5.

Zhengyu Zhu received B.S. degree from Henan University in 2010. He is currently pursuing the Ph.D. degree in communications with the School of Information Engineering, Zhengzhou University China. Since 2013, he has been visiting Korea University, Seoul, South Korea, where he has been conducting collaborative research as a Visiting Student. His research interests include information theory and signal processing for wireless communications such as MIMO wireless network, physical layer security, wireless cooperative networks, convex optimization techniques, and energy harvesting communication systems.

Zheng Chu received the Ph.D. degree from the School of Electrical and Electronic Engineering, Newcastle University, U.K., in 2016. He is currently with the School of Science and Technology, Middlesex University. His research interests include physical layer security, wireless cooperative networks, wireless power transfer, convex optimization techniques, and game theory.

Zhongyong Wang received the B.S. and M.S. degrees in automatic control from the Harbin Shipbuilding Engineering Institute, Harbin, China, in 1986 and 1988, respectively, and the Ph.D. degree in automatic control theory and application from Xi'an Jiaotong University, Xi'an, China, in 1998. Since 1988, he has been with the Department of Electronics, Zhengzhou University, Zhengzhou, China, as a Lecturer. From 1999 to 2002, he was an Associate Professor, where he was promoted to Professor with the Department of Communication Engineering in 2002. His general fields of interest cover numerous aspects within embedded systems, signal processing, and communication theory.

Inkyu Lee received the B.S. (Hons.) degree in control and instrumentation engineering from Seoul National University, Seoul, South Korea, in 1990, and the M.S. and Ph.D. degrees in electrical engineering from Stanford University, Stanford, CA, USA, in 1992 and 1995, respectively. From 1995 to 2001, he was a member of Technical Staff with Bell Laboratories, Lucent Technologies, where he studied high-speed wireless system designs. From 2001 to 2002, he was with Agere Systems, Murray Hill, NJ, USA, as a Distinguished Member of Technical Staff. Since 2002, he has been with Korea University, Seoul, where he is currently a Professor with the School of Electrical Engineering. In 2009, he visited the University of Southern California, Los Angeles, CA, USA, as a Visiting Professor. He has authored over 130 journal papers in the IEEE. He has 30 U.S. patents granted or pending. His research interests include digital communications, signal processing, and coding techniques applied for nextgeneration wireless systems. He has served as an Associate Editor of the IEEE TRANSACTIONS ON COMMUNICATIONS from 2001 to 2011, and the IEEE TRANSACTIONS ON WIRELESS COMMUNICATIONS from 2007 to 2011. He has been a Chief Guest Editor of the IEEE JOURNAL ON SELECTED AREAS IN COMMUNICATIONS (Special Issue on 4G Wireless Systems) in 2006. He was a recipient of the IT Young Engineer Award at the IEEE/IEEK Joint Award in 2006, and of the Best Paper Award at APCC in 2006, the IEEE VTC in 2009, and ISPACS in 2013. He was also a recipient of the Best Research Award from the Korea Information and Communications Society in 2011, and the Best Young Engineer Award from the National Academy of Engineering in Korea (NAEK) in 2013. He has been elected as a member of NAEK in 2015. He is an IEEE fellow.